Am J Transl Res 2021;13(11):12536-12548
www.ajtr.org /ISSN:1943-8141/AJTR0130877

Original Article

Myosin 1b promotes migration, invasion and glycolysis in cervical cancer via ERK/HIF-1α pathway

Li-Jun Wen[1,2], Xiao-Lin Hu[1], Cui-Ying Li[1,2], Jie Liu[3], Zi-Yang Li[1], Ya-Zi Li[1], Jue-Yu Zhou[1]

[1]Department of Biochemistry and Molecular Biology, School of Basic Medical Sciences, Southern Medical University, Guangzhou 510515, Guangdong, China; [2]School of Basic Medical Sciences, Southern Medical University, Guangzhou 510515, Guangdong, China; [3]Department of Gynaecology and Obstetrics, Nanfang Hospital, Southern Medical University, Guangzhou 510515, Guangdong, China

Received January 26, 2021; Accepted August 21, 2021; Epub November 15, 2021; Published November 30, 2021

Abstract: Background: Increasing evidence indicated that metabolic reprograming is essential and has been regarded as a hallmark of cancer. Although the biological functions of Myosin 1b (Myo1b) have been reported in several malignancies, the correlation between Myo1b and cancer metabolism, and its underlying mechanisms remain elusive, particularly in cervical cancer (CC). Methods: Myo1b and other glycolytic enzymes expression levels were examined in CC cells and tumor tissues from xenograft models by quantitative real-time PCR, Western blot and immunohistochemistry. The biological impacts and regulatory mechanisms of Myo1b on cell migration, invasion and glycolysis were explored. Also, the effects of Myo1b on carcinogenesis and metastasis in nude mice were investigated. Results: Upregulation of Myo1b was found in CC tissues and associated with poor prognosis. Overexpressed Myo1b not only significantly elevated CC cell glycolysis, migration and invasion in vitro, but also promoted tumorigenesis and metastasis in vivo. Conversely, Myo1b knockdown had opposite consequences. Moreover, our study suggested that Myo1b stimulated ERK/HIF-1α pathway and its downstream glycolysis associated genes to modulate the glycolysis, migration and invasion of CC. Conclusion: These findings provide evidence that Myo1b regulates migration, invasion and glycolysis in CC through ERK/HIF-1α pathway, suggesting a promising remedial target in treatment of CC.

Keywords: Myosin 1b, cervical cancer, ERK/HIF-1α, glycolysis, invasion, metastasis

Introduction

As the fourth most common gynecological malignancy globally, cervical cancer (CC) poses a serious health threat to women [1]. In accordance with global cancer statistics in 2018, there were estimated 570,000 new cases of CC with 311,000 deaths [2]. Despite the fact that availability and improvement in HPV vaccination and early screening of HR-HPV have contributed to the reduction in the incidence and mortality rates of CC, treatments for those patients who have advanced and recurrent CC remain unsatisfactory [3]. Therefore, targeted therapy has been considered as a promising strategy for CC [4], and it is also necessary to identify metastasis-related biomarkers and therapeutic targets for CC.

Disorder of cellular metabolism is involved in cancer genesis and progression [5]. The metabolic change from the mitochondrial tricarboxylic acid (TCA) cycle to aerobic glycolysis is the major metabolism-related trait of most cancer cells [6]. That is, even in aerobic conditions, glucose is absorbed in large quantities and transformed to lactate by the glycolytic route in tumor cells. This phenomenon is a hallmark of tumor cell metabolism, termed as the Warburg effect (aerobic glycolysis) [7]. It provides proliferative and survival advantages as well as acidic microenvironments for the tumor that may in turn promote cancer epithelial-mesenchymal transition (EMT) and migration [8, 9]. Hypoxia-inducible factor-1α (HIF-1α) acts as a transcription factor, is one of the primary glycolytic regulators [10]. The glycolytic proteins, glucose

transporter 1 (GLUT1), hexokinase 2 (HK2), phosphoglycerate kinase 1 (PGK1), lactate dehydrogenase A (LDHA) and pyruvate kinase M (PKM) are genes induced by HIF-1α [11, 12]. It has been reported that extracellular signal-regulated kinase (ERK) pathway, essential for extracellular stimuli responses, is a crucial regulator of glycolysis [13]. Zhao *et al.* [14] demonstrated that ERK/HIF-1α pathway has a great influence on the genesis of progressive fibrosis. More importantly, Wang *et al.* [15] has found that EGFR/MEK/ERK pathway increases the HIF-1α expression to regulate metabolism in pancreatic cancer, suggesting the potential for interrupting the EGFR/MEK/ERK/HIF-1α pathway in cancer treatment. Therefore, gaining a better understanding of this process and exploring the underlying target genes are crucial for identifying new potential targets and developing novel effective therapeutic strategies for CC.

Myosin 1b (Myo1b) is one class of single-headed, actin-related molecular motor and extensively expressed in mammalian tissues [16]. According to localization and subcellular fractionation researches, Myo1b may associate with the cytomembrane and a few subcellular organelles, for instance lysosomes and endosomes [16]. Emerging evidences indicate that Myo1b function as a key oncogenic driver in carcinogenesis, including head and neck squamous cell carcinoma (HNSCC) [17], prostate cancer [18] and glioma [19]. Our previous research has shown that Myo1b is distinctly upregulated in CC tissues and cells. We also demonstrated that Myo1b could have an important effect on cervical tumorigenesis by influencing cell motility, migration and invasion, which suggested that Myo1b might be used as a therapeutic target for CC [20]. However, the underlying mechanism of Myo1b in regulating carcinogenesis has not been completely clarified.

In the present research, we aimed to figure out the influence of Myo1b on migration and invasion, and further unravel the function of Myo1b in modulating metabolic mechanisms in CC. We revealed that enhanced Myo1b expression facilitated CC cell migration and invasion, and the activity of key glucose metabolizing enzymes in vitro and in vivo. Mechanistically, Myo1b promoted glycolysis by stimulating the ERK/HIF-1α pathway. We report for the first time the role of Myo1b in regulating the Warburg effect in cervical carcinogenesis.

Materials and methods

Bioinformatic data mining

Kaplan-Meier plotter database analysis: Expression analysis and survival curves with *P* value were plotted with the Kaplan-Meier plotter (http://kmplot.com/analysis/) [21]. It enables us to investigate the impact (expression, survival and biomarkers) of 54 k genes in 21 cancer types, including 304 cases of cervical cancer by the web tool. We detected the Myo1b expression in normal and CC tissues, and assessed the survival outcomes of CC in different expression levels of Myo1b.

Gene set enrichment analysis (GSEA): We identified genes related to specific biological states using the GSEA [22]. GSEA v3.0 (http://www.broadinstitute.org/gsea/) with gene sets from the Molecular Signatures Database (MSigDB) (http://software.broadinstitute.org/gsea/msigdb) was used to analyze association between Myo1b signaling pathway and biological processes gene sets. The relation of Myo1b expression with biological function was analyzed using the gene set of HALLMARK_GLYCOLYSIS. Statistical significance was defined as false discovery rate <0.25 and *P*-value of <0.05.

The c-Bio cancer genomics portal (c-BioPortal): It (http://www.cbioportal.org/) [23] is an integrated online tool containing information from TCGA, GEO and several cancer genome databases. It allows us to search for DNA mutations, DNA methylation, mRNA or miRNA expression change, clinical data and co-expression of the genes conveniently. We explored the co-expressed genes of Myo1b by the "co-expression" column of c-BioPortal.

Cell culture and compounds

The CaSki, SiHa and C33A human cervical cancer cell lines were obtained from the Cell Bank of Chinese Academy of Sciences (Shanghai, China). The CC cells were cultured in Dulbecco's Modified Eagle Medium (DMEM, Life Technologies, Shanghai, China) with 10% fetal bovine serum (FBS, Gibco, CA, USA) at 37°C and 5% CO_2. The cobalt chloride ($CoCl_2$, Sigma-Aldrich,

MO, USA) was used to mimic hypoxia conditions and U0126 (MedChemExpress, NJ, USA) was applied to inhibit ERK signaling.

Plasmid transfection and siRNA interference

To obtain Myo1b overexpression, we constructed the full-length of Myo1b (NM_001161819) in pcDNA3.1 vector by FulenGen (Guangzhou, China). To silence Myo1b expression, small interfering RNAs that targeted Myo1b (si-Myo1b) were bought from GenePharma (Shanghai, China). The negative controls were empty vector (pcDNA3.1) or scramble siRNA (si-NC). Following the manufacturer's instructions, cells were transfected by Lipofectamine 2000 (Invitrogen, CA, USA) for 4 h when cell confluency reached 60-80%. The transfected cells were collected for further studies after 48-72 h. The details of the siRNA sequences were provided in Table S1.

Stable cell line generation

The synthesized short hairpin RNA targeting Myo1b (sh-Myo1b) or control shRNAs (sh-NC) were bought from GeneChem (Shanghai, China). SiHa cells were transfected with sh-Myo1b and control using Lipofectamine 2000 (Invitrogen, CA, USA). After selecting transfected cells by 700 μg/ml Geneticin for 4 weeks, the transfected cells were collected, verified by Western blot, and used for the foundation of xenografted nude mice models. The sequences used for shRNA were presented in Table S2.

Transwell migration and invasion assays

Before conducting migration and invasion assay, cells were treated with hypoxia-mimetic agent $CoCl_2$. For cell migration assays, 3×10^5 cells were seated in the upper chambers. In the lower chambers, 600 μl DMEM with 20% FBS was added while medium without FBS was added in the upper chambers. The paraformaldehyde was used to fix the migrated cells for 20 min, then the cells were stained with 0.1% crystal violet for 20 min and finally imaged under a microscope after 24 h incubation. The number of total cells of invasion assay is 5×10^5 cells per chamber and cells were coated with matrigel in upper chamber (Corning, MA, USA). The main step of cell invasion assay was close to the assay of cell migration. To access the cell migration and invasion ability, the numbers of cells that invaded through the pores were counted and calculated by selecting five fields of view at random.

Quantitative real-time PCR

Total RNAs from cells treated with $CoCl_2$ were isolated by RNAiso Plus reagent (Takara, Shiga, Japan), and then the Prime-Script kit (TaKaRa, Dalian, China) was utilized for the cDNA synthesis. The SYBR Premix Ex Taq kit (TaKaRa, Dalian, China) was used to examine the specific gene expressions by an ABI 7500 Real-Time PCR system. The PCR reaction was performed as follows: 40 cycles with 5 s at 95°C and 34 s at 60°C after pre-denaturation 30 s at 95°C. And a final step of the procedure is at 95°C for 15 s, 60°C for 1 min. The relative gene expression quantification was conducted using the $2^{-\Delta\Delta CT}$ method. The primer sequences are shown in Table S3.

Western blot assay

Cells were cultivated with 10 μM $CoCl_2$. Then the RIPA buffer containing protease inhibitors was used to lyse cells and a BCA protein assay reagent kit (Beyotime Biotechnology, Shanghai, China) was used to quantify the proteins extracted from cells. Equal amount of proteins was separated onto an 8% sodium dodecyl sulfate-polyacrylamide gel electrophoresis and transferred onto a polyvinylidene fluoride membrane (Millipore Corporation, Billerica, USA). The membrane was incubated with primary antibodies at 4°C overnight after blocking with 5% non-fat milk. Antibody against Myo1b (1:3,000; Abcam, Cambridge, USA), HIF-1α (1:1,000; Cell Signaling Technology, Danvers, USA), p-ERK (1:500), ERK (1:1,000), LDHA (1:5,000), HK2 (1:5,000), GLUT1 (1:1,000), PKM (1:1,000), β-actin (1:3,000) (all from Proteintech Group, Chicago, USA) were used. Then we incubated the membrane with the secondary antibody (1:3,000; Proteintech Group, Chicago, USA) for 2 h in room temperature. The Image-J software and enhanced chemiluminescence ECL detection Kit (Millipore Corporation, Billerica, USA) were used to visualize and quantify the signals.

In vivo xenografted nude mice models

The animal experiments were implemented in 4-week-old female BALB/c nude mice (Beijing HFK Bioscience Co. Ltd, China), and performed in accordance with the guidelines of Use and

Care of Laboratory Animals (Southern Medical University, Guangzhou, China). To evaluate the tumorigenicity of Myo1b in vivo, 5×10^6 sh-Myo1b or control shRNA SiHa cells mixed with matrigel (Corning, MA, USA) and PBS were injected into right flank of the mice (n=6 per group). The sizes of tumors were measured using a caliper every 3 days and tumor volumes were calculated with the formula: Length × Width^2 × 0.5. Then, the mice were raised till the 30th day and euthanized in CO_2 chamber, followed by cervical dislocation before the neoplasms were surgically resected. To establish the lung metastasis model, 1×10^5 sh-Myo1b or control shRNA SiHa cells with PBS were injected into tail vein of the mice (n=4 per group). After 4 weeks, the mice were sacrificed equally and metastatic nodules were verified by H&E staining. In addition, immunohistochemistry staining was performed on the tumors using antibodies against HIF-1α (Cell Signaling Technology, Danvers, USA), Ki-67, LDHA and PKM (Proteintech Group, Chicago, USA), respectively.

Immunohistochemical staining (IHC)

Paraffin-embedded tissue sections were deparaffinized with dimethylbenzene and rehydrated in ethanol, followed by antigen retrieval in 0.01 M sodium citrate buffer solution. Following inhibition of endogenous peroxidase in 3% H_2O_2 for 15 min and blocking using bovine serum albumin (Amresco, Ohio, USA) for 1 h, the sections were incubated with primary antibodies against HIF-1α (Cell Signaling Technology, Danvers, USA), Ki-67, LDHA and PKM (Proteintech Group, Chicago, USA) at 4°C overnight. Then the sections were incubated with the secondary antibody at room temperature for 30 min, stained with 3, 3'-diaminobenzidine (DAB; ZSGB-BIO, Beijing, China), and finally counter-stained using hematoxylin (Beyotime Biotechnology, Shanghai, China). Representative slices were chosen and the positive staining areas (%) were measured by Image J software (NIH, USA).

Statistical analysis

The biochemical experiments were carried out in triplicate, and all data were shown as mean ± SD. The differences between groups in vitro and in vivo analyses were defined using two-tailed unpaired Student's t test or one-way ANOVA. Multiple comparisons between the groups were performed using ANOVA followed by the LSD post hoc test. The SPSS 23.0 software (IBM, Chicago, USA) was used to analyze all the data, and *P* values <0.05 were regarded as statistically significant.

Results

Expression and clinical significance of Myo1b in CC

We utilized the Kaplan Meier-plotter database to make a comparison of Myo1b expression levels between CC and normal tissues, aiming to determinate the Myo1b expression and its clinical significance in CC. It revealed that compared to the normal tissues, Myo1b was significantly upregulated in CC tissues (**Figure 1A**). Quantitative analysis for Kaplan-Meier overall survival curves in low and high Myo1b expression CC cases in the database indicated that elevated Myo1b expression is correlated with poor overall survival distinctly (**Figure 1B**). We validated that Myo1b is markedly unregulated in CC and its high expression is related to poor survival by analyzing public CC gene expression datasets.

Myo1b enhances CC cell migration and invasion in vitro and in vivo

To understand Myo1b's role in CC aggressive phenotype, we investigated whether altering Myo1b expression influences the cell migration and invasion abilities. Therefore, Myo1b was silenced or overexpressed by siRNA (shRNA) or Myo1b overexpression vector transfection, respectively. After transfection with Myo1b siRNA (shRNA) or pcDNA3.1-Myo1b vectors, Myo1b was decreased in CaSki and SiHa cells or increased in C33A cells (**Figure 2A**). Compared to the control, suppressing Myo1b expression resulted in significantly decreased number of migrated and invaded CC cells (**Figure 2B**). On the contrary, upregulating Myo1b expression markedly increased the cell migration and invasion in C33A cells (**Figure 2C**). Furthermore, we injected Myo1b-suppressed or control SiHa cells into the caudal vein of mice to assess the impact of Myo1b on cell metastasis in vivo. The nodules from sh-Myo1b group were fewer and smaller than those in control group (**Figure 2D**). Together, these data highlight that Myo1b could have an important impact on invasion and metastasis of CC cells.

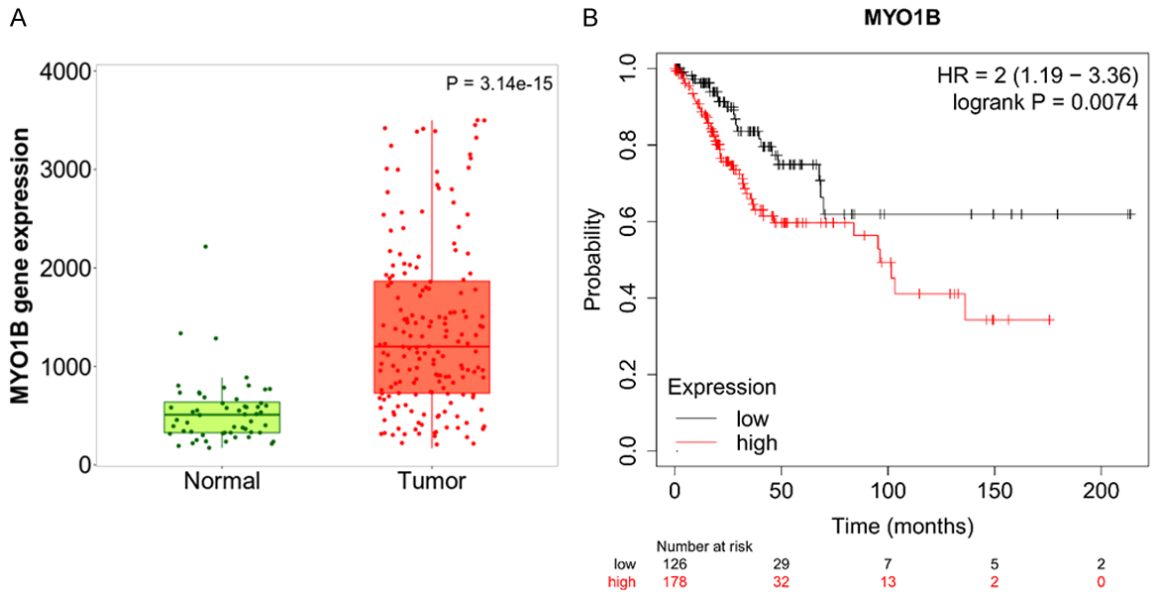

Figure 1. Myo1b is overexpressed in CC and related to poor prognosis. A. The box plot showed Myo1b expression in tumor tissues (n=189) (right plot) and normal tissues (n=56) (left plot) analyzed with the Kaplan Meier-plotter database. B. Elevated Myo1b expression is related to poor overall survival (OS) in CC patients. The Kaplan-Meier Plotter database was used to acquire and analyze the prognosis data.

Myo1b regulates pathways associated with glucose metabolism in CC cells

The gene set enrichment analysis (GSEA) of 308 CC cases from TCGA data was conducted for further investigation into the molecular mechanism of Myo1b in CC tumorigenesis. And the results showed a relationship between Myo1b expression and increased glycolytic metabolism in CC on account of conspicuous changes in metabolic processes containing upregulation of glycolysis (NES=1.42, P<0.05, **Figure 3A**). Then we explored whether Myo1b triggers glycolysis changes in CC by detecting the mRNA expression of 13 glycolytic genes (HIF-1α, GLUT1, HK2, GPI, PFKL, TPI, GAPDH, ALDOA, PGK1, PGAM2, ENO1, PKM2 and LDHA) using real-time qualitative PCR. Consistently, majority of metabolic enzymes included in glycolysis (HIF-1α, GLUT1, HK2, GPI, GAPDH, ALDOA, PGK1, PKM2 and LDHA) were significantly downregulated by Myo1b knockdown in both SiHa and CaSki cells (**Figure 3B**). Further analysis indicated that Myo1b expression positively correlated with other glycolytic genes including HIF-1α, GLUT1, PKM, LDHA and HK2 in TCGA database (**Figure 3C**). Next, we detected the protein levels of GLUT1, PKM, LDHA, HK2, and observed that Myo1b knocked down only reduced PKM and HK2 expression in CaSki and SiHa cells (**Figure 3D**). To reveal the signaling pathway involved in the effect of Myo1b on glycolysis, we examined the activity of ERK/HIF-1α pathway, which is known to be associated with glucose metabolism. Silencing Myo1b inhibited p-ERK and HIF-1α expression compared with the control group, indicating that Myo1b could activate ERK/HIF-1α pathway (**Figure 3D**). These results signified that Myo1b was associated with cervical carcinogenesis by modulating aerobic glycolysis.

U0126 partially reverses the oncogenic activities of Myo1b in CC

As mentioned above, our studies have demonstrated that Myo1b promotes cell migration and invasion, and increases the activity of key glucose metabolizing enzymes, which may be related to the ERK/HIF-1α pathway stimulation. To validate the dependency of Myo1b-mediated oncogenic activities on this pathway, we used the ERK pathway inhibitor U0126 to block it. As shown in **Figure 4A**, increased Myo1b expression resulted in ERK/HIF-1α signaling activation, which in turn elevated the expression of GLUT1, PKM and LDHA, and was counteracted by the treatment of U0126. In addition, Myo1b overexpression enhanced the malignant transformation abilities of C33A such as cell migration and invasion, which could be reversed by U0126 (**Figure 4B**). In conclusion, these results

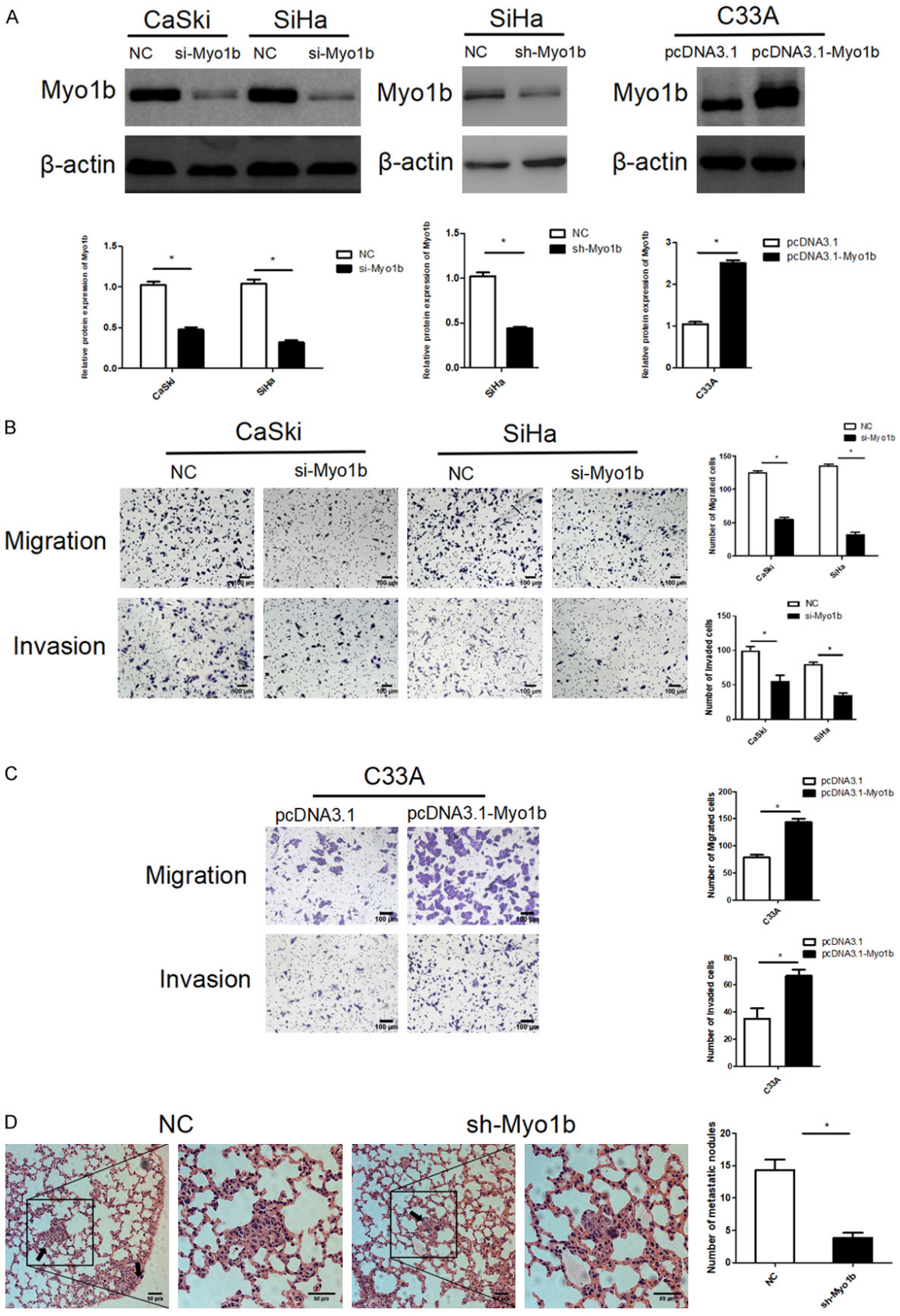

Figure 2. Myo1b promotes cell migration and invasion in vitro and in vivo. A. Western blot analysis for validation of Myo1b knockdown and overexpression in CC cell lines. B. Myo1b knockdown blocked the migration and invasion

of CC cells. C. Overexpressed Myo1b enhanced the migration and invasion of C33A cells. The number of cells per field was counted. Scale bar =100 μm. D. The microscopic presentation of staining with H&E (200× and 400×) and quantification of the lung metastasis. Scale bar =50 μm. Data are shown as mean ± SD. The experiments were repeated for at least three times (*P<0.05).

A

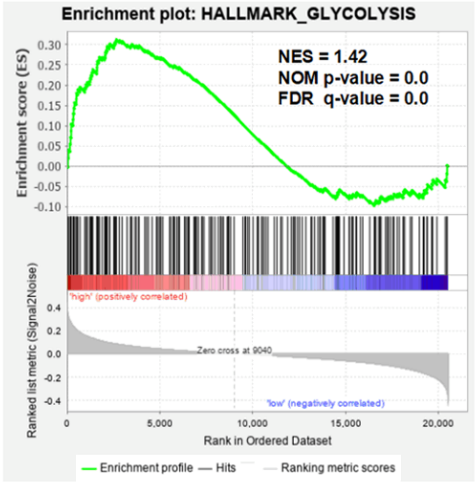

B

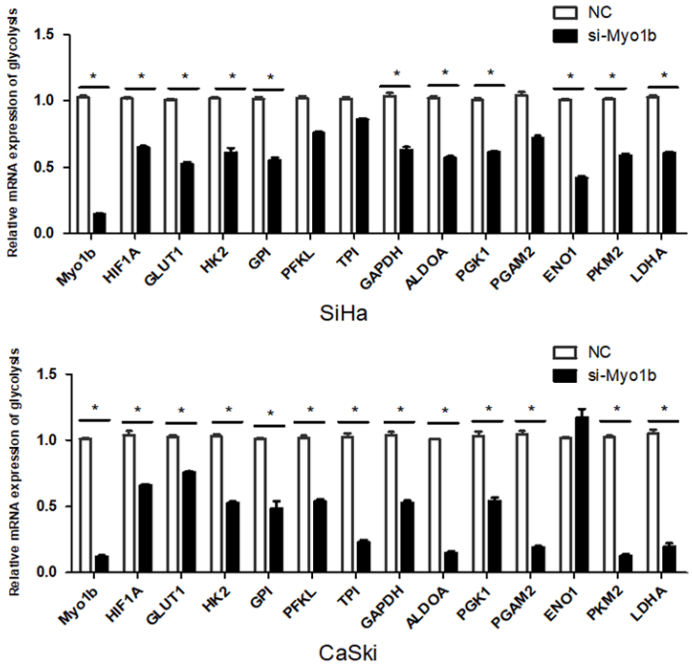

C

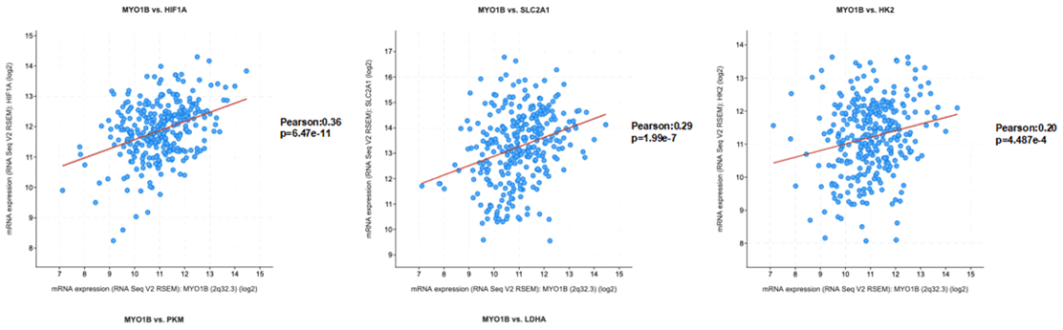

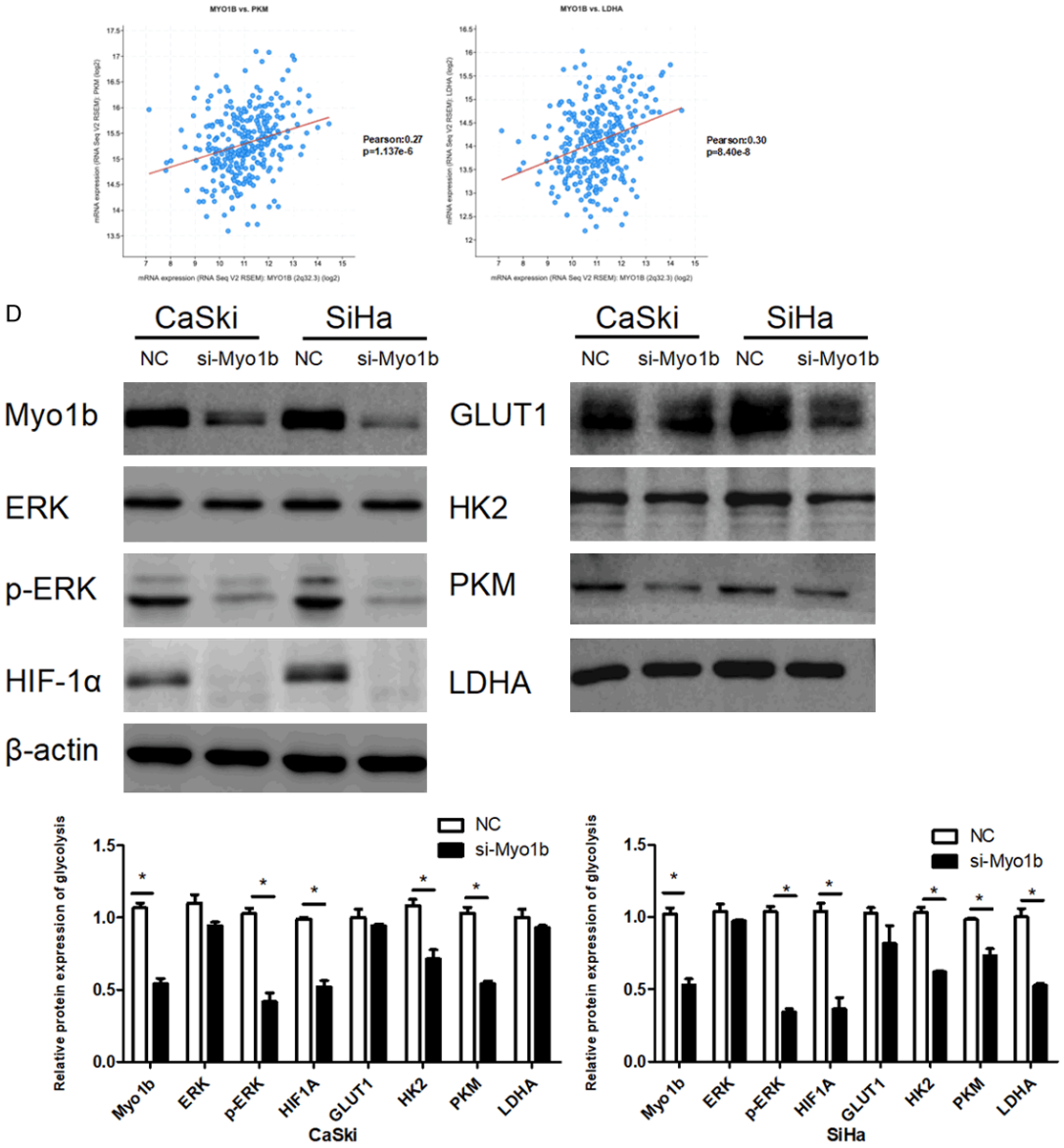

Figure 3. Myo1b depletion inhibits glycolysis in CC cells. A. Gene sets enrichment analysis showed that the gene sets of HALLMARK_GLYCOLYSIS were enriched in the group with overexpressed Myo1b. NES, normalized enrichment score; NOM, nominal; FDR, false discovery rate. B. mRNA levels of glycolysis-related genes after silencing Myo1b expression in SiHa cells and CaSki cells. C. Correlation analysis of the expression between Myo1b and glycolysis-related genes including HIF-1α, GLUT1, HK2, PKM and LDHA in TCGA database. D. Western blot analysis of GLUT1, PKM, LDHA, HK2, ERK, p-ERK and HIF-1α protein expressions in si-Myo1b or si-NC CC cells. Data are presented as mean ± SD for three independent experiments (*P<0.05).

showed that inhibition of the ERK pathway abolished the effect of Myo1b overexpression on C33A malignant behaviors, indicating the important roles of ERK/HIF-1α in Myo1b mediated cervical carcinogenesis.

Silencing of Myo1b inhibits xenograft cervical tumor growth in nude mice

Next, we explored the role of Myo1b in carcinogenesis using the nude mice xenograft model. SiHa cells with sh-NC or sh-Myo1b were subcutaneously injected into nude mice. Our results revealed that tumors derived from sh-Myo1b group were smaller and lighter than those in sh-NC group (**Figure 5A**). IHC staining for Ki-67 revealed that tumor tissues in the sh-Myo1b group showed lower positivity rate than those in the control group (**Figure 5B**). Additionally, we found that the Myo1b-silencing tumor tissues showed lower HIF-1α, PKM and LDHA expres-

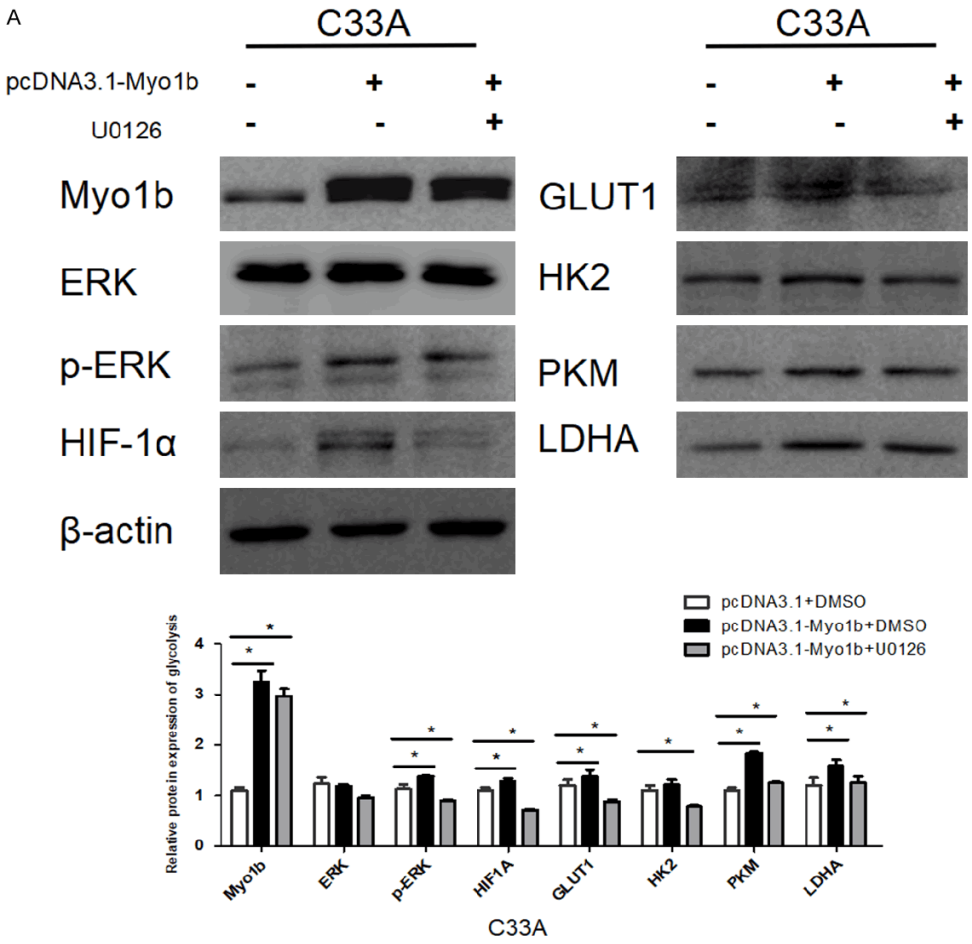
A
C33A
C33A
pcDNA3.1-Myo1b
U0126
Myo1b
ERK
p-ERK
HIF-1α
β-actin
GLUT1
HK2
PKM
LDHA
pcDNA3.1+DMSO
pcDNA3.1-Myo1b+DMSO
pcDNA3.1-Myo1b+U0126
Relative protein expression of glycolysis
Myo1b
ERK
p-ERK
HIF1A
GLUT1
HK2
PKM
LDHA
C33A

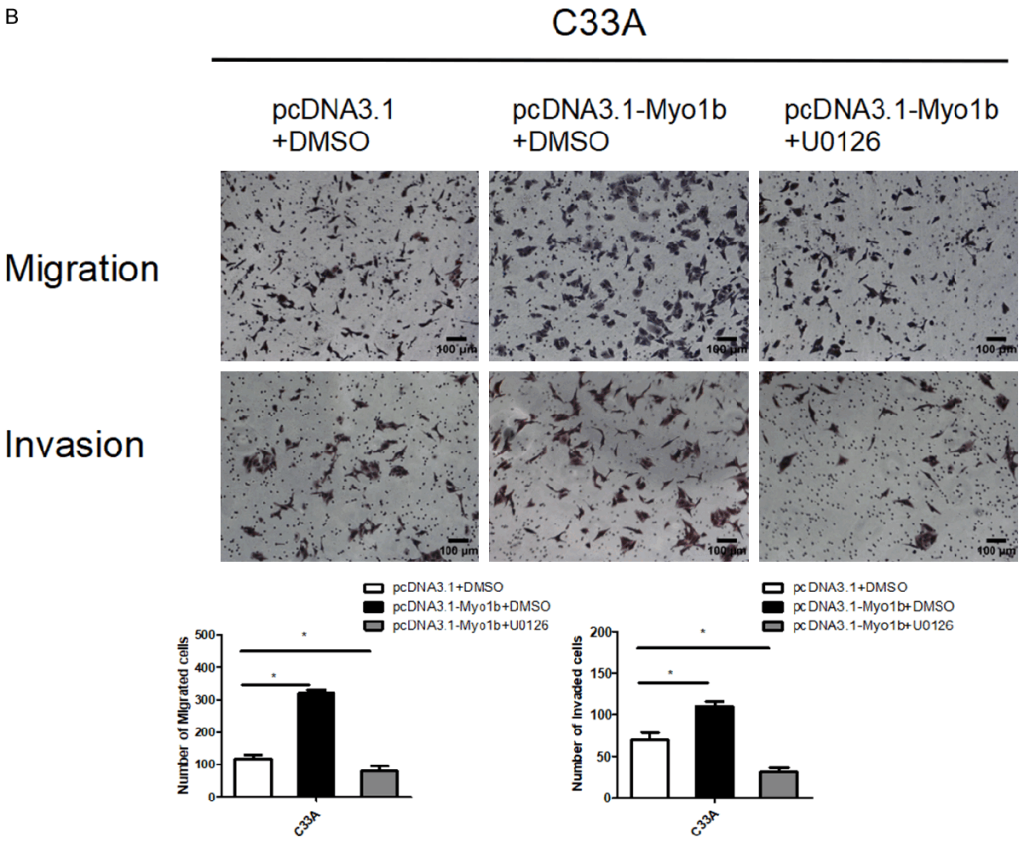
B
C33A
pcDNA3.1 +DMSO
pcDNA3.1-Myo1b +DMSO
pcDNA3.1-Myo1b +U0126
Migration
Invasion
pcDNA3.1+DMSO
pcDNA3.1-Myo1b+DMSO
pcDNA3.1-Myo1b+U0126
Number of Migrated cells
C33A
Number of Invaded cells
C33A

Figure 4. U0126 partially reverses the oncogenic activities of Myo1b in CC. A. Western blot analysis of GLUT1, PKM, LDHA, HK2, ERK, p-ERK and HIF-1α protein levels in Myo1b-overexpressed C33A cells with or without treatment of U0126. B. Overexpression of Myo1b enhances the migration and invasion abilities of C33A, which could be reversed by U0126. Scale bar =100 μm. Data are shown as mean ± SD, *P<0.05. The experiments were independently repeated three times.

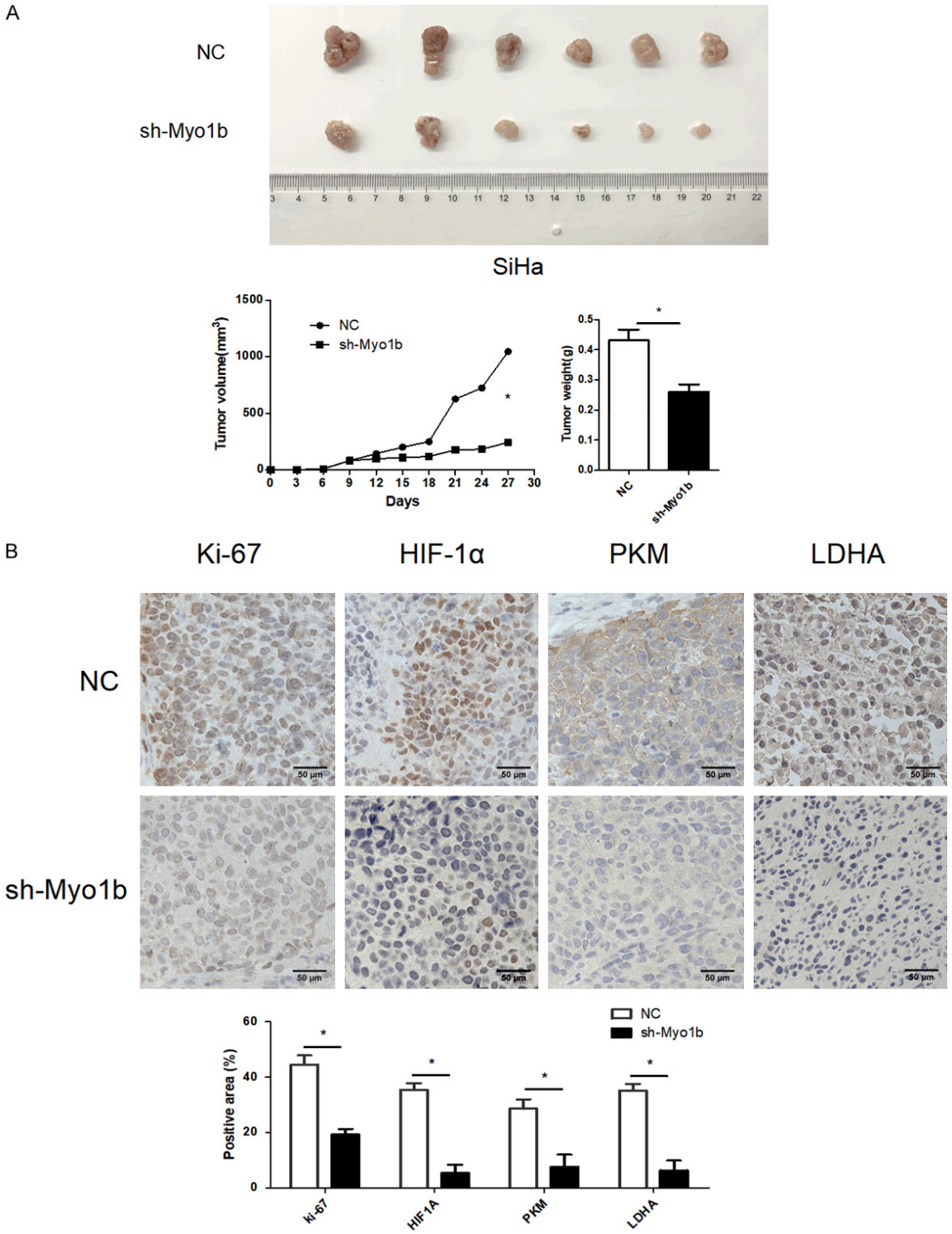

Figure 5. Silencing of Myo1b inhibits the tumorigenicity and glycolysis in vivo. A. Influence of Myo1b on tumor volume, growth and weight in vivo (N=6 per group). B. IHC staining of Ki-67, HIF-1α, PKM and LDHA in tumor specimens

from xenografts (400×). The positively stained area (%) was quantified in three fields for three independent tumors. Scale bar is 50 μm. All the data are shown as mean ± SD; *P<0.05.

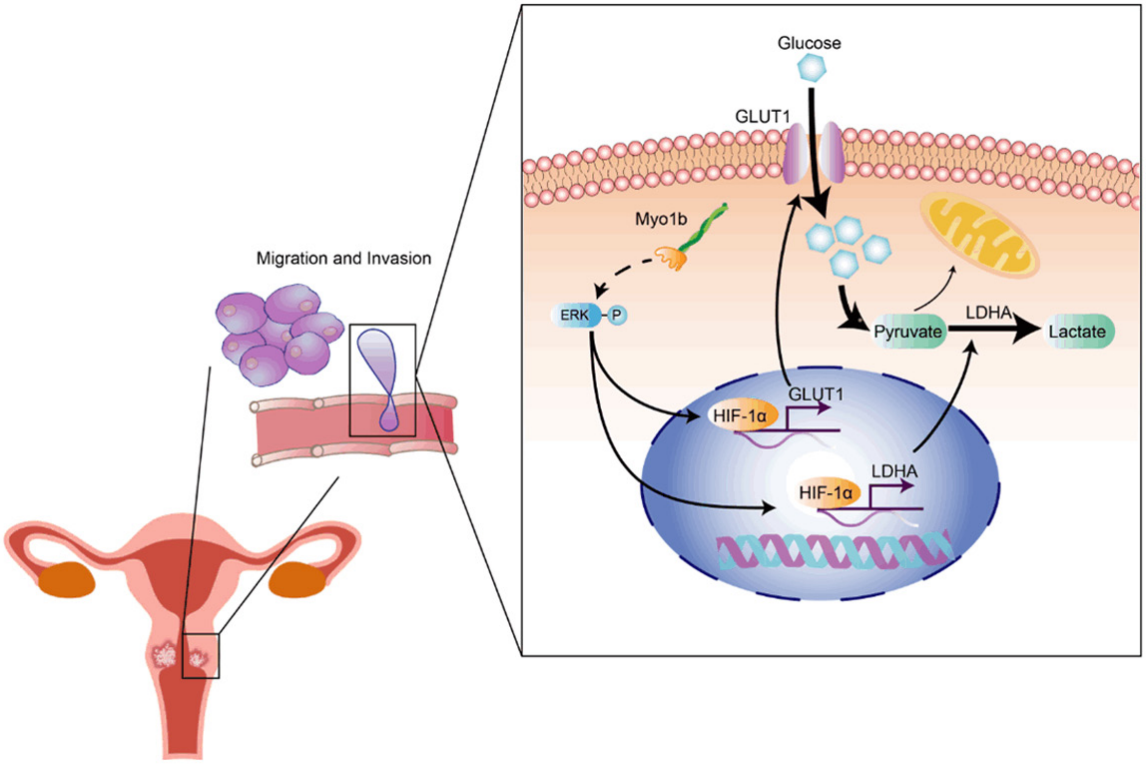

Figure 6. Schematic diagram showing that upregulation of Myo1b activates ERK/HIF-1α signaling pathways, thereby promoting cell migration, invasion and glycolysis.

sion, substantiating that Myo1b promotes CC by regulating these important glucose metabolism factors. **Figure 6** summarized the molecular mechanism and function of Myo1b in this study.

Discussion

Inhibition of glycolysis has been proven to suppress tumor growth [24] and increase radiosensitivity in cervical cancer cells [25], indicating the important implications of glycolysis to cervical cancer. Emerging evidence has demonstrated that Myo1b was overexpressed and promoted tumor progression in several cancers, including prostate cancer and HNSCC [17, 18]. However, the role of Myo1b and its regulatory mechanism in glycolysis have rarely been discussed. This research reported for the first time that Myo1b-mediated modulation of glucose metabolism could be a target for cervical cancer prevention and therapy.

Mounting evidences have demonstrated that Myo1b could act as a tumor promoter by activating some cellular pathways. It has been reported that Myo1b recruited PI3K to stimulate PDK1/AKT and PAK/LIMK pathways in glioma [19]. Moreover, another recent study revealed that Myo1b suppressed cell apoptosis by regulating AKT activation [26]. Nevertheless, we found that Myo1b promoted cell migration, invasion and glycolysis in CC by phosphorylating ERK pathway. Previous studies indicated that ERK pathway could play a vital role in cervical cancer tumorigenesis [27, 28]. Furthermore, ERK pathway could activate the central regulator HIF-1α, which modulates the genes that code for glycolytic enzymes and enzymes that convert glucose into lactate, causing increased aerobic glycolysis [29, 30]. Consistent with these studies, our results found that activation of ERK1/2 pathways by Myo1b elevated expression levels of HIF-1α and its targets (GLUT1 and LDHA). Rescue experiments further sup-

ported that suppression of ERK/HIF-1α pathway in Myo1b-overexpressed cells repressed the abilities of cell invasion and migration. Besides, Myo1b expression was positively related to HIF-1α expression in tumor xenografts. Our findings will, with no doubt, enrich the mechanism of how Myo1b regulates CC cells migration, invasion and glycolysis.

Although our findings for the first time indicated the potential roles of Myo1b in glycolysis via regulating ERK/HIF-1α pathway in CC, there are still some limitations in the current study. First, the underlying mechanism of how Myo1b activates the ERK pathway still needs to be explored. Thus, Co-IP assay and mass spectrometry are warranted to find out the interaction between Myo1b and its partners. Second, it should be noted that we confirmed the involvement of Myo1b in the process of glycolysis in CC, but other mechanisms are not excluded. Whether Myo1b-mediated tumorigenesis is involved in angiogenesis, drug resistance and radiotherapy resistance needs further studies.

In summary, we found that upregulation of Myo1b could predict poor survival of cervical cancer patients. Functional studies showed that Myo1b promoted migration, invasion and glycolysis via stimulation of the ERK/HIF-1α pathway. Thus, our results uncovered a novel function of Myo1b in regulating glucose metabolism which provides a novel and prospective therapeutic target in cervical cancer.

Acknowledgements

This research was supported by the grants from the National Natural Science Foundation of China (81972755, 81672588, 31900886), the Natural Science Foundation of Guangdong Province (2020A1515011278, 2018A03031-3392) and the National Undergraduate Training Program for Innovation and Entrepreneurship (201812121002, S201912121057).

Disclosure of conflict of interest

None.

Address correspondence to: Jue-Yu Zhou, Department of Biochemistry and Molecular Biology, School of Basic Medical Sciences, Southern Medical University, No. 1023-1063, Shatai South Road, Baiyun District, Guangzhou 510515, China. Tel: 020-61648209; E-mail: zhoujueyu@126.com

References

[1] Arbyn M, Weiderpass E, Bruni L, de Sanjose S, Saraiya M, Ferlay J and Bray F. Estimates of incidence and mortality of cervical cancer in 2018: a worldwide analysis. Lancet Glob Health 2020; 8: e191-e203.

[2] Bray F, Ferlay J, Soerjomataram I, Siegel RL, Torre LA and Jemal A. Global cancer statistics 2018: GLOBOCAN estimates of incidence and mortality worldwide for 36 cancers in 185 countries. CA Cancer J Clin 2018; 68: 394-424.

[3] Hu Z and Ma D. The precision prevention and therapy of HPV-related cervical cancer: new concepts and clinical implications. Cancer Med 2018; 7: 5217-5236.

[4] Crafton SM and Salani R. Beyond chemotherapy: an overview and review of targeted therapy in cervical cancer. Clin Ther 2016; 38: 449-458.

[5] Hanahan D and Weinberg RA. Hallmarks of cancer: the next generation. Cell 2011; 144: 646-674.

[6] Wang H, Zhou R, Sun L, Xia J, Yang X, Pan C, Huang N, Shi M, Bin J, Liao Y and Liao W. TOP-1MT deficiency promotes GC invasion and migration via the enhancements of LDHA expression and aerobic glycolysis. Endocr Relat Cancer 2017; 24: 565-578.

[7] Warburg O. On the origin of cancer cells. Science 1956; 123: 309-314.

[8] Vander Heiden MG, Cantley LC and Thompson CB. Understanding the Warburg effect: the metabolic requirements of cell proliferation. Science 2009; 324: 1029-1033.

[9] Lu J, Tan M and Cai Q. The Warburg effect in tumor progression: mitochondrial oxidative metabolism as an anti-metastasis mechanism. Cancer Lett 2015; 356: 156-164.

[10] Marin-Hernandez A, Gallardo-Perez JC, Ralph SJ, Rodriguez-Enriquez S and Moreno-Sanchez R. HIF-1alpha modulates energy metabolism in cancer cells by inducing over-expression of specific glycolytic isoforms. Mini Rev Med Chem 2009; 9: 1084-1101.

[11] Semenza GL. HIF-1 mediates metabolic responses to intratumoral hypoxia and oncogenic mutations. J Clin Invest 2013; 123: 3664-3671.

[12] Zhao W, Chang C, Cui Y, Zhao X, Yang J, Shen L, Zhou J, Hou Z, Zhang Z, Ye C, Hasenmayer D, Perkins R, Huang X, Yao X, Yu L, Huang R, Zhang D, Guo H and Yan J. Steroid receptor coactivator-3 regulates glucose metabolism in bladder cancer cells through coactivation of hypoxia inducible factor 1alpha. J Biol Chem 2014; 289: 11219-11229.

[13] Papa S, Choy PM and Bubici C. The ERK and JNK pathways in the regulation of metabolic

reprogramming. Oncogene 2019; 38: 2223-2240.
[14] Zhao Y, Ma X, Wang J, He X, Hu Y, Zhang P, Wang R, Li R, Gong M, Luo S and Xiao X. Curcumin protects against CCl4-induced liver fibrosis in rats by inhibiting HIF-1alpha through an ERK-dependent pathway. Molecules 2014; 19: 18767-18780.
[15] Wang G, Li Y, Yang Z, Xu W, Yang Y and Tan X. ROS mediated EGFR/MEK/ERK/HIF-1alpha loop regulates glucose metabolism in pancreatic cancer. Biochem Biophys Res Commun 2018; 500: 873-878.
[16] Komaba S and Coluccio LM. Localization of myosin 1b to actin protrusions requires phosphoinositide binding. J Biol Chem 2010; 285: 27686-27693.
[17] Ohmura G, Tsujikawa T, Yaguchi T, Kawamura N, Mikami S, Sugiyama J, Nakamura K, Kobayashi A, Iwata T, Nakano H, Shimada T, Hisa Y and Kawakami Y. Aberrant myosin 1b expression promotes cell migration and lymph node metastasis of HNSCC. Mol Cancer Res 2015; 13: 721-731.
[18] Makowska KA, Hughes RE, White KJ, Wells CM and Peckham M. Specific myosins control actin organization, cell morphology, and migration in prostate cancer cells. Cell Rep 2015; 13: 2118-2125.
[19] Zhou X, Wang R, Li X, Yu L, Hua D, Sun C, Shi C, Luo W, Rao C, Jiang Z, Feng Y, Wang Q and Yu S. Splicing factor SRSF1 promotes gliomagenesis via oncogenic splice-switching of MYO1B. J Clin Invest 2019; 129: 676-693.
[20] Zhang HR, Lai SY, Huang LJ, Zhang ZF, Liu J, Zheng SR, Ding K, Bai X and Zhou JY. Myosin 1b promotes cell proliferation, migration, and invasion in cervical cancer. Gynecol Oncol 2018; 149: 188-197.
[21] Nagy A, Munkacsy G and Gyorffy B. Pancancer survival analysis of cancer hallmark genes. Sci Rep 2021; 11: 6047.
[22] Subramanian A, Tamayo P, Mootha VK, Mukherjee S, Ebert BL, Gillette MA, Paulovich A, Pomeroy SL, Golub TR, Lander ES and Mesirov JP. Gene set enrichment analysis: a knowledge-based approach for interpreting genome-wide expression profiles. Proc Natl Acad Sci U S A 2005; 102: 15545-15550.
[23] Cerami E, Gao J, Dogrusoz U, Gross BE, Sumer SO, Aksoy BA, Jacobsen A, Byrne CJ, Heuer ML, Larsson E, Antipin Y, Reva B, Goldberg AP, Sander C and Schultz N. The cBio cancer genomics portal: an open platform for exploring multidimensional cancer genomics data. Cancer Discov 2012; 2: 401-404.
[24] Liu Y, Murray-Stewart T, Casero RA Jr, Kagiampakis I, Jin L, Zhang J, Wang H, Che Q, Tong H, Ke J, Jiang F, Wang F and Wan X. Targeting hexokinase 2 inhibition promotes radiosensitization in HPV16 E7-induced cervical cancer and suppresses tumor growth. Int J Oncol 2017; 50: 2011-2023.
[25] Rashmi R, Huang X, Floberg JM, Elhammali AE, McCormick ML, Patti GJ, Spitz DR and Schwarz JK. Radioresistant cervical cancers are sensitive to inhibition of glycolysis and redox metabolism. Cancer Res 2018; 78: 1392-1403.
[26] Yu Y, Xiong Y, Ladeiras D, Yang Z and Ming XF. Myosin 1b regulates nuclear AKT activation by preventing localization of PTEN in the nucleus. iScience 2019; 19: 39-53.
[27] Wan PK, Leung TH, Siu MK, Mo XT, Tang HW, Chan KK, Cheung AN and Ngan HY. HPV-induced Nurr1 promotes cancer aggressiveness, self-renewal, and radioresistance via ERK and AKT signaling in cervical cancer. Cancer Lett 2021; 497: 14-27.
[28] Li S, Ma YM, Zheng PS and Zhang P. GDF15 promotes the proliferation of cervical cancer cells by phosphorylating AKT1 and Erk1/2 through the receptor ErbB2. J Exp Clin Cancer Res 2018; 37: 80.
[29] Marampon F, Gravina GL, Zani BM, Popov VM, Fratticci A, Cerasani M, Di Genova D, Mancini M, Ciccarelli C, Ficorella C, Di Cesare E and Festuccia C. Hypoxia sustains glioblastoma radioresistance through ERKs/DNA-PKcs/HIF-1alpha functional interplay. Int J Oncol 2014; 44: 2121-2131.
[30] Wan J and Wu W. Hyperthermia induced HIF-1a expression of lung cancer through AKT and ERK signaling pathways. J Exp Clin Cancer Res 2016; 35: 119.

Table S1. Sequences for siRNAs

siRNA	Sequences (5'-3')
si-Myo1b	CUUGUUGAUUUCCAGGUAAGC
	GCUUACCUGGAAAUCAACAAG
NC	UUCUCCGAACGUGUCACGU
	ACGUGACACGUUCGGAGAA

Table S2. Sequences for shRNAs

shRNA	Sequences (5'-3')
sh-Myo1b	GATCCCGCTTACCTGGAAATCAACAAGCTCGAGCTTGTTGATTTCCAGGTAAGCTTTTTGGAT
	AGCTATCCAAAAAGCTTACCTGGAAATCAACAAGCTCGAGCTTGTTGATTTCCAGGTAAGCGG
NC	CCGGTTCTCCGAACGTGTCACGTTTCAAGAGAACGTGACACGTTCGGAGAATTTTTG
	AATTCAAAAATTCTCCGAACGTGTCACGTTCTCTTGAAACGTGACACGTTCGGAGAA

Table S3. The primers used in qRT-PCR analysis

Gene	Sense and antisense primer (5'-3')
Myo1b	GCTCTGGTGTGGAGGTCCTA
	CGTTGCTTCCTCAGGTCTTC
HIF-1α	CCATTAGAAAGCAGTTCCGC
	TGGGTAGGAGATGGAGATGC
GLUT1	TTGGCTCCGGTATCGTCAAC
	GCCAGGACCCACTTCAAAGA
LDHA	CCAGCGTAACGTGAACATCTT
	CCCATTAGGTAACGGAATCG
ENO1	GTGTGGCTCTAACCCTCTGG
	TCTGTGACGTTCAGTTTCTTGC
PKM2	GAACTTCTCTCATGGAACTCAT
	GATCTCAGGTCCTTTAGTGTCTA
PGAM2	AGAAGCACCCCTACTACAACTC
	TCTGGGGAACAATCTCCTCGT
HK2	GCCATCCTGCAACACTTAGGGCTTGAG
	GTGAGGATGTAGCTTGTAGAGGGTCCC
ALDOA	ATGCCCTACCAATATCCAGCA
	GCTCCCAGTGGACTCATCTG
PGK1	GAACAAGGTTAAAGCCGAGCC
	GTGGCAGATTGACTCCTACCA
GPI	CAAGGACCGCTTCAACCACTT
	CCAGGATGGGTGTGTTTGACC
PFKL	GGTGCCAAAGTCTTCCTCAT
	GATGATGTTGGAGACGCTCA
TPI1	AGCTCATCGGCACTCTGAAC
	CCACAGCAATCTTGGGATCT
GAPDH	GCACCGTCAAGGCTGAGAAC
	TGGTGAAGACGCCAGTGGA
β-actin	CATGTACGTTGCTATCCAGGC
	CTCCTTAATGTCACGCACGAT